inorganics

MDPI

Article

Design and Construction of a Mixed-Ligand Coordinated Fluorescent Complex and Its Application for Sensing Ions, Antibiotics, and Pesticides in Aqueous Solution

Gao-Sheng Zhu [1], Yi Jia [2], Jia-Yao Ding [1], Hao Yin [1], Yan Chen [1], Bao-Yi Yu [1,*], Yan-Ying Zheng [1,*] and Francis Verpoort [3,4,*]

[1] Key Laboratory of Urban Agriculture in North China, Ministry of Agriculture P.R. China, College of Bioscience and Resources Environment, Beijing University of Agriculture, Beijing 102206, China; zhugaoshengbua@163.com (G.-S.Z.); yyqx17710825739@163.com (J.-Y.D.); 202230121128@bua.edu.cn (H.Y.); cheny@bua.edu.cn (Y.C.)
[2] CAS Key Lab of Colloid, Interface and Chemical Thermodynamics, Institute of Chemistry, Chinese Academy of Sciences, Beijing 100190, China; jiayi@iccas.ac.cn
[3] State Key Laboratory of Advanced Technology for Materials Synthesis and Processing, Wuhan University of Technology, Wuhan 430070, China
[4] Research School of Chemical and Biomedical Technologies, National Research Tomsk Polytechnic University, Lenin Avenue 30, 634050 Tomsk, Russia
* Correspondence: baoyi.yu@bua.edu.cn (B.-Y.Y.); huaxue@bua.edu.cn (Y.-Y.Z.); francis@whut.edu.cn (F.V.); Tel.: +86-135-1106-6021 (B.-Y.Y.)

Table S1. Crystal data for Complex Zn.

CCDC No.	2082189
Formula	$C_{42}H_{33.6}N_{14}O_{10.8}Zn$
Formula weight	972.60
Temperature/K	150.0(1)
Crystal system	Triclinic
Space group	Pī
a / Å	6.833(1)
b / Å	9.549(1)
c / Å	16.521(3)
α / °	94.292(4)
β / °	96.712(5)
γ / °	104.117(5)
V / Å^3	1032.2(3)
Z	1
ρ_{calc}[g/cm^3]	1.65
μ / mm^{-1}	0.677
F(000)	500.0
Crystal size/mm^3	0.27 × 0.21 × 0.2
Radiation	MoK*α* (λ = 0.71073)
2θ range for data collection / °	4.424 to 52.892
Index ranges	$-8 \le h \le 8, -11 \le k \le 11, -20 \le l \le 20$
Reflections collected	11184

Independent reflections	4202 [R_{int} = 0.0914, R_{sigma} = 0.1334]
Data/restraints/parameters	4202/380/369
Goodness-of-fit on F^2	1.038
Final R indexes [I >=2σ (I)][a]	R_1 = 0.0719, wR_2 = 0.1293
Final R indexes [all data][b]	R_1 = 0.1554, wR_2 = 0.1630
Largest diff. peak/hole / e Å^{-3}	0.53/-0.67

[a] $R_1 = \Sigma_1|F_0|-|F_C|/\Sigma_1|F_0|$; [b] $wR_2 = [\Sigma[w(F_0^2-F_C^2)^2]/\Sigma[(F_0^2)^2]]^{1/2}$.

Table S2. The selected bond lengths [Å] and angles [°] for Complex Zn.

Atoms	**Bond length [Å]**	**Atoms**	**Bond length[Å]**	**Atoms**	**Bond length[Å]**	**Atoms**	**Bond length[Å]**
Zn1O1	2.115(3)	N5C18	1.414(6)	C2C7	1.3900	C18C19	1.376(6)
Zn1O1$^{\#1}$	2.115(3)	N5C20	1.333(6)	C2C3	1.3900	C18C17	1.382(7)
Zn1O1W$^{\#1}$	2.117(4)	N5N6	1.41(2)	C7C8	1.446(6)	N3C14	1.28(4)
Zn1O1W	2.117(4)	O4C12	1.22(2)	N2N3	1.357(5)	N6C21	1.32(3)
Zn1N1$^{\#1}$	2.109(4)	C15C19	1.384(6)	N2C15	1.424(6)	C8C9	1.372(8)
Zn1N1	2.109(4)	C15C16	1.375(6)	N2C13	1.337(6)	C11C10	1.374(9)
O1C1	1.263(6)	C1C2	1.518(5)	N4C17	1.338(6)	C9C10	1.388(9)
O2C1	1.263(6)	C12C5	1.518(5)	N4C16	1.331(6)	C4C3	1.3900
N1C13	1.327(6)	C6C7	1.3900	O3C12	1.31(2)	C5C4	1.3900
N1C14A	1.34(3)	C6C5	1.3900	N7C20	1.25(8)		
N1C14	1.40(3)	C6C11	1.493(6)	N7C21	1.4(1)		
Atoms	**Bond angle** [°]	**Atoms**	**Bond angle** [°]	**Atoms**	**Bond angle** [°]	**Atoms**	**Bond angle** [°]
O1Zn1O1$^{\#1}$	180.0(2)	N1Zn1N1$^{\#1}$	180.0	C2C7C6	120.0	C19C15N2	119.6(4)
O1Zn1O1W$^{\#1}$	92.4(1)	C1O1Zn1	130.9(3)	C2C7C8	119.7(3)	C16C15N2	120.1(4)
O1Zn1O1W	87.6(1)	C13N1Zn1	128.2(3)	C8C7C6	120.2(3)	C16C15C19	120.3(4)
O1$^{\#1}$Zn1O1W$^{\#1}$	87.6(1)	O2C1C2	118.1(4)	C20N5N6	108(1)	C18C19C15	117.5(5)
O1$^{\#1}$Zn1O1W	92.4(1)	N7C20N5	113(5)	N6N5C18	119(1)	C21N6N5	101(2)
O1WZn1O1W$^{\#1}$	180.0	O3C12C5	112.9(9)	N3N2C15	120.7(4)	C9C8C7	121.1(6)
N1$^{\#1}$Zn1O1$^{\#1}$	91.0(1)	O4C12O3	123(1)	C13N2N3	110.1(4)	C10C11C6	121.9(6)
N1$^{\#1}$Zn1O1	89.0(1)	O4C12C5	123.9(8)	C13N2C15	129.3(4)	C8C9C10	120.9(6)
N1Zn1O1	91.0(1)	C7C6C5	120.0	C16N4C17	119.2(4)	C11C10C9	119.8(6)
N1Zn1O1$^{\#1}$	89.0(1)	C7C6C11	116.0(3)	C20N7C21	103(8)	N6C21N7	113(5)
N1Zn1O1W$^{\#1}$	94.3(2)	C5C6C11	124.0(3)	C19C18N5	120.7(4)	N3C14N1	116(1)
N1$^{\#1}$Zn1OW$^{\#1}$	85.7(2)	C7C2C1	120.8(3)	C19C18C17	119.7(4)	C3C4C5	120.0
N1$^{\#1}$Zn1O1W	94.3(2)	C3C2C1	119.1(3)	C17C18N5	119.6(4)	C2C3C4	120.0
N1Zn1O1W	85.5(2)	C3C2C7	120.0	C4C5C6	120.0	O1C1C2	116.8(4)
C13N1C14	100(1)	N4C16C15	121.5(4)	N4C17C18	121.7(5)	O1C1O2	125.0(5)
C14N1Zn1	131(1)	C6C5C12	121.9(3)	N1C13N2	110.4(4)		
C20N5C18	130.7(4)	C4C5C12	118.1(3)	C14N3N2	102.3(7)		

Symmetry transformation: #1 1-x, 1-y, 1-z.

Table S3. Chemical structure of the selected antibiotics.

Kind	Name (abbreviation)	Chemical structure
Lactams	Benzylpenicillin potassium (PK)	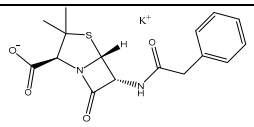
	Penicillin V potassium (PVK)	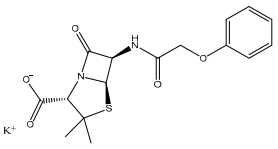
	Amoxicillin (AML)	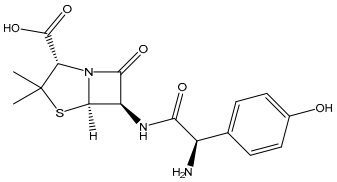
	Cefixime (CFX)	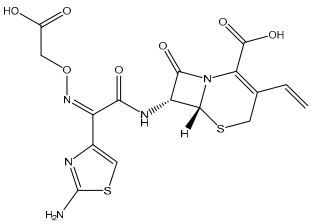
Aminoglycosides	Gentamicin (GTM)	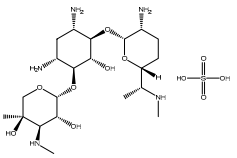
	Kanamycin (KNM)	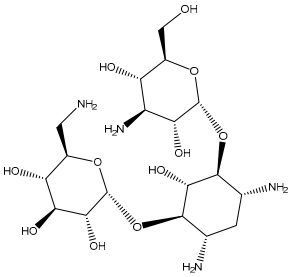
	Tobramycin (TOB)	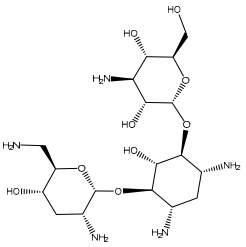

Chloramphenicols	Streptomycin (SM)	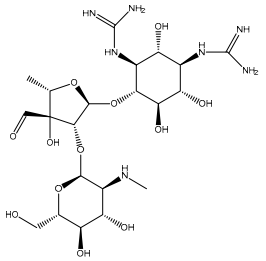
	Chloramphenicol (CAP)	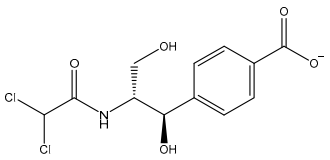
	Thiamphenicol (TAP)	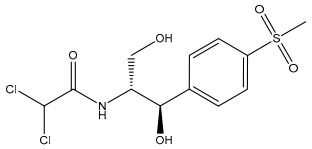
Macrolides	Roxithromycin (ROX)	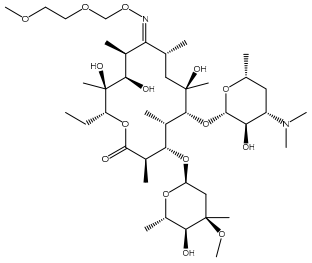
	Azithromycin (AZM)	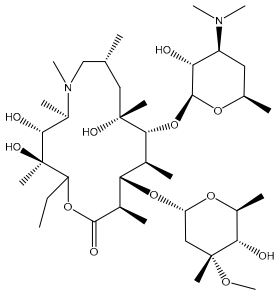
Nitrofurans	Nitrofurantoin (NFT)	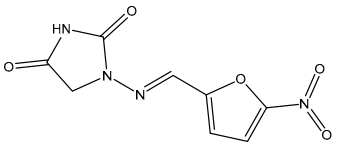
	Nitrofurazone (NFZ)	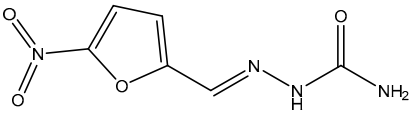
Nitroimidazoles	Metronidazole (MNZ)	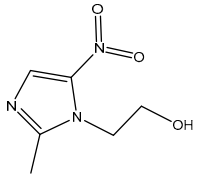
	1,2-dimethyl-5-nitroimidazole (DMZ)	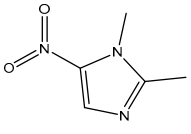

Sulfonamides	Sulfamethazine (SMZ)	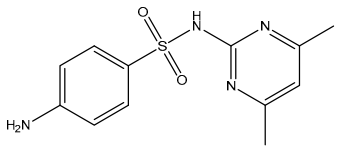

Table S4. Chemical structure of the selected pesticides.

Name (abbreviation)	Chemical structure
Dipterex (DIP)	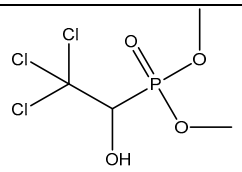
Pentachloro-nitrobenzene (PCNB)	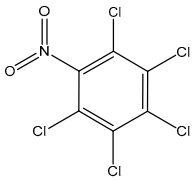
Imazalil (IMZ)	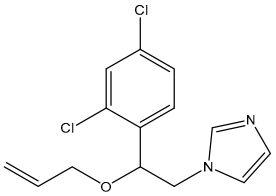
Glyphosate (GLY)	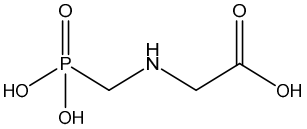
Chlorothalonil (TPN)	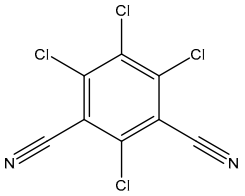
Carbendazim (CAR)	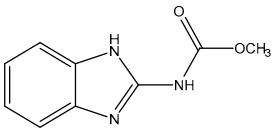
2,4-dichlorophenoxyacetic acid (2,4-D)	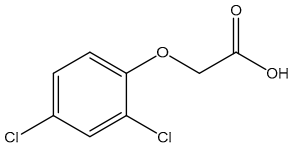
Imidacloprid (IMI)	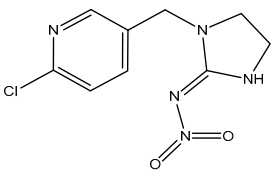

Metamitron (MMT)

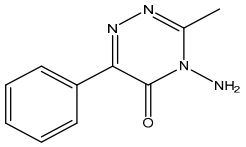

Thiophanate-methyl (TPM)

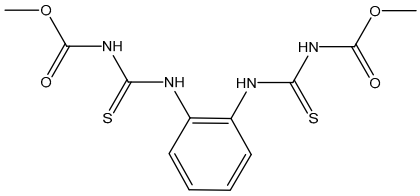

Nitenpyram (NTP)

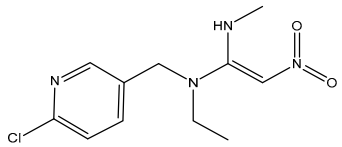

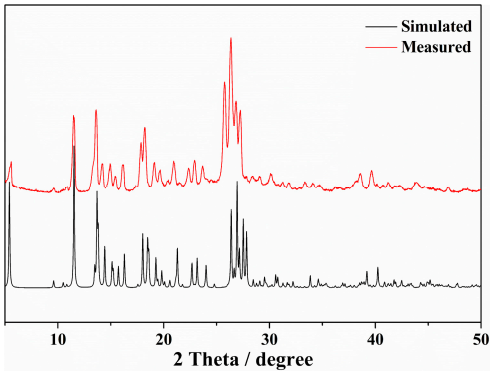

Figure S1. PXRD patterns of Complex Zn (as synthesized and simulated).

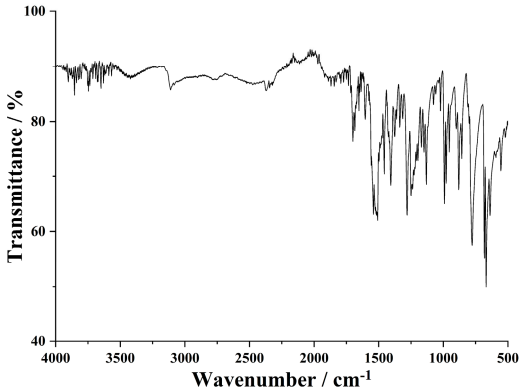

Figure S2. FT-IR spectrum of Complex Zn.

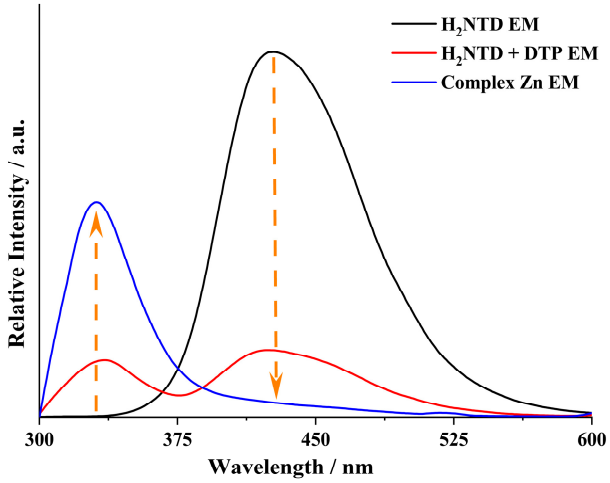

Figure S3. Emission spectra (excitation at 259 nm) of H_2NTD, H_2NTD + DTP, and Complex Zn.

It is well known that complexes bearing an H_2NTD ligand exhibit excellent fluorescent properties[33,34]. Figure 4 shows that the presence of free H_2NTD led to strong emission, and the intensity of the peak decreased upon the addition of an equal amount of free DTP. Under this condition, almost equal intensities which were contributed by the two ligands were observed. However, with the incorporation of the two ligands in Complex Zn, the emission of the H_2NTD ligand was clearly diminished by the DTP ligand. It has been observed that charge-transfer processes, specifically ligand-ligand electron (charge) transfer (LLCT), may occur during photo-irradiation in the presence of CPs bearing electron-rich carboxylic-containing ligands and conjugated *N*-heterocyclic ligands such as polypyridine-derivatives, pyrazine-derivatives, or polyimidazole-derivatives [35]. Additionally, an alternative pathway for electron transfer (ET) may involve proton-coupled electron transfer (PECT), particularly when a hydrogen bond (N–H···O) is present within the product structure, formed between anionic carboxylate and protonated 4,4′-bipyridine species [36]. Notably, in Complex Zn's structure, an evident hydrogen bond exists between $HNTD^-$ and DTP ligands (refer to Figure 1c). A plausible scenario involves a PECT process where the carboxylic group acts as the electron donor, and the pyridyl moiety of the DTP ligand acts as the electron acceptor. Furthermore, the π···π stacking within the structure of Complex Zn may facilitate electron transfer from $HNTD^-$ to DTP, thereby reducing excitation energy [37]. Hence, the observed decrease in $HNTD^-$ emission by DTP in Complex Zn during the fluorescence process can be attributed to ET.

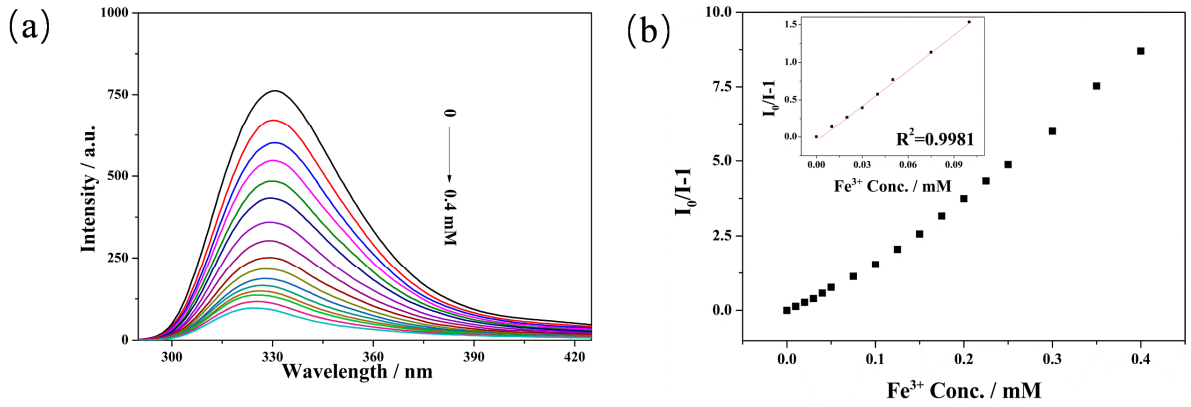

Figure S4. Fluorescence intensities of Complex Zn (a) dispersed in different concentrations of Fe^{3+}; the plot of I_0/I - 1 of Complex Zn (b) *vs*. concentration of Fe^{3+} in aqueous solution (Inset: The plot of I_0/I - 1 of the Complex Zn with the concentration over a Fe^{3+} concentration range of 0-0.10 mM in aqueous solution).

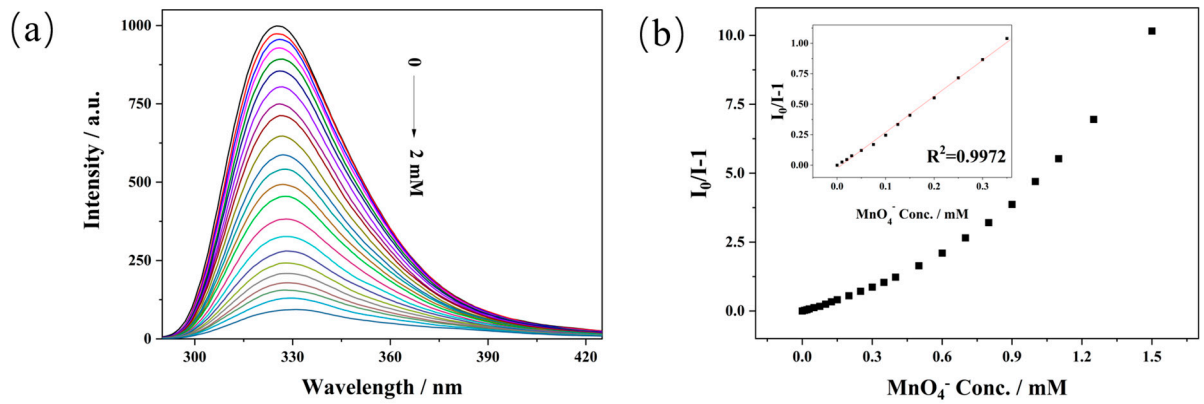

Figure S5. Fluorescence intensities of Complex Zn (a) dispersed in different concentrations of MnO_4^-; the plot of I_0/I - 1 of Complex Zn (b) *vs*. concentration of MnO_4^- in aqueous solution (Inset: The plot of I_0/I - 1 of the Complex Zn with the concentration over a MnO_4^- concentration range of 0 - 0.35 mM in aqueous solution).

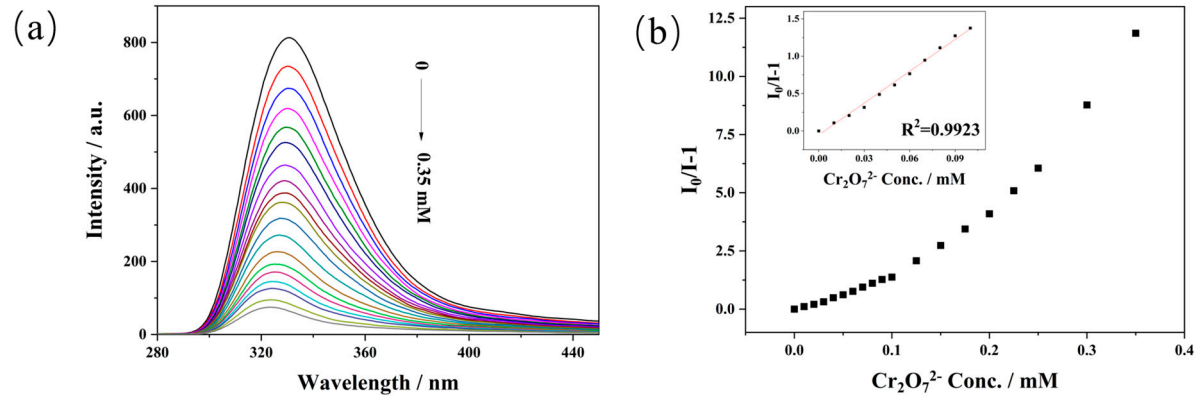

Figure S6. Fluorescence intensities of Complex Zn (a) dispersed in different concentrations of $Cr_2O_7^{2-}$; the plot of I_0/I - 1 of Complex Zn (b) *vs*. concentration of $Cr_2O_7^{2-}$ in aqueous solution (Inset: The plot of I_0/I - 1 of the Complex Zn with the concentration over a $Cr_2O_7^{2-}$ concentration range of 0-0.10 mM in aqueous solution).

Table S5. K_{sv} and LODs values of Complex Zn for ions detection.

Sensor	Analyte	Concentration / mg·mL^{-1}	Linear range / μM	LOD / μM	$K_{sv} \times 10^4$ / M^{-1}
Complex Zn	Fe^{3+}	0.1	0-100	0.60	1.55
Complex Zn	MnO_4^-	0.1	0-350	0.76	1.21
Complex Zn	$Cr_2O_7^{2-}$	0.1	0-100	0.56	1.64

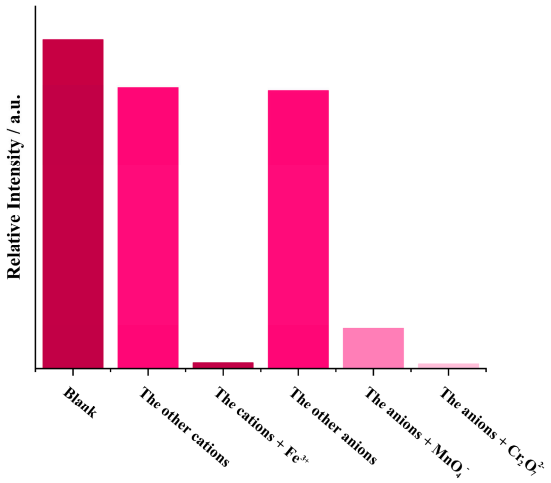

Figure S7. Fluorescent intensity of Complex Zn in the presence of other cations and anions (The other cations = K^+, Na^+, Mg^{2+}, Ca^{2+}, Ni^{2+}, Co^{2+}, Mn^{2+}, Cu^{2+}, Zn^{2+}, Cd^{2+}, Pb^{2+}, Ba^{2+}, Al^{3+}, Cr^{3+} and Fe^{3+}; The other anions = F^-, Cl^-, Br^-, I^-, Ac^-, SCN^-, NO_3^-, ClO_3^-, ClO_4^-, HPO_4^{2-}, $H_2PO_4^-$, CO_3^{2-}, $B_4O_7^{2-}$, SO_3^{2-} and SO_4^{2-}), before and after addition of Fe^{3+}, MnO_4^- or $Cr_2O_7^{2-}$.

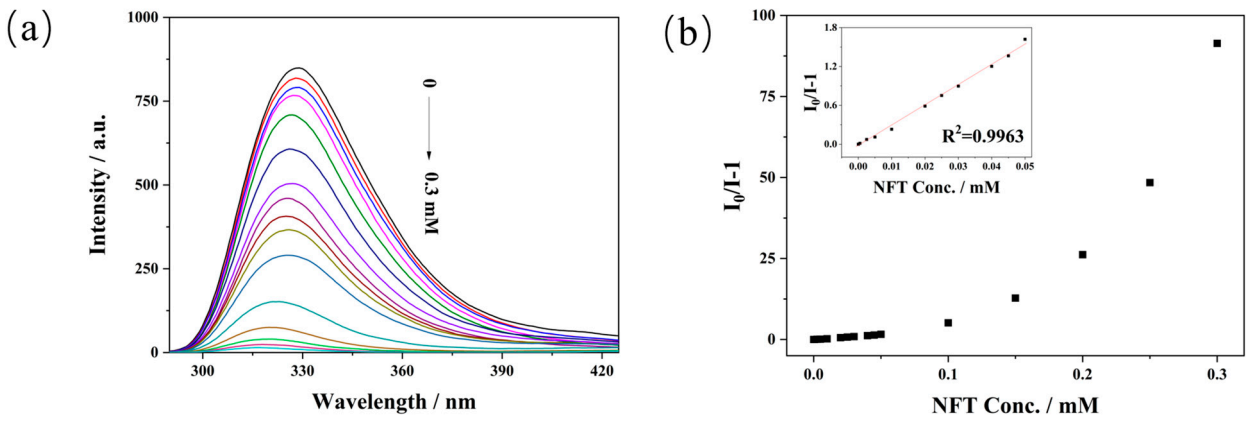

Figure S8. Fluorescence intensities of Complex Zn (a) dispersed in different concentrations of NFT; the plot of I_0/I - 1 of Complex Zn (b) *vs*. concentration of NFT in aqueous solution (Inset: The plot of I_0/I - 1 of the Complex Zn with the concentration over a NFT concentration range of 0-0.05 mM in aqueous solution).

Table S6. K_{sv} and LOD values for recently reported lanthanide CP-based luminescence probes for sensing of NFT.

Sensor	Analyte	Concentration / mg·mL^{-1}	Linear range / μM	LOD / μM	$K_{sv} \times 10^4$ / M^{-1}	Ref.
Complex Zn	NFT	0.1	0-50	0.40	2.34	This work
{[Zn(TTPBA-4)$_{0.5}$(TPA)]·H_2O·0.5DMF}$_n$	NFT	-	0-10	-	2.00	[40]
{[Zn(L)]·CH_3CN}$_n$	NFT	0.6	-	3.28	2.48	[41]
RhB@ZIF-8	NFT	0.8	0-38	0.47	1.80	[42]
FSS@ZIF-8	NFT	0.8	0-38	0.35	2.00	[43]
{[Zn_2(TRZ)$_2$(DBTDC-O_2)]·DMAc}$_n$	NFT	1.0	4-20	0.35	18.00	[44]
[$Zn_8(C_5H_4N_5)_4(C_{14}H_8O_4)_6O(C_{50}H_{44}N_4)_{0.5}$]	NFT	0.5	-	0.56	4.42	[44]
{[Zn(tptc)$_{0.5}$(bimb)] ·H_2O}$_n$	NFT	0.5	-	0.49	4.51	[45]

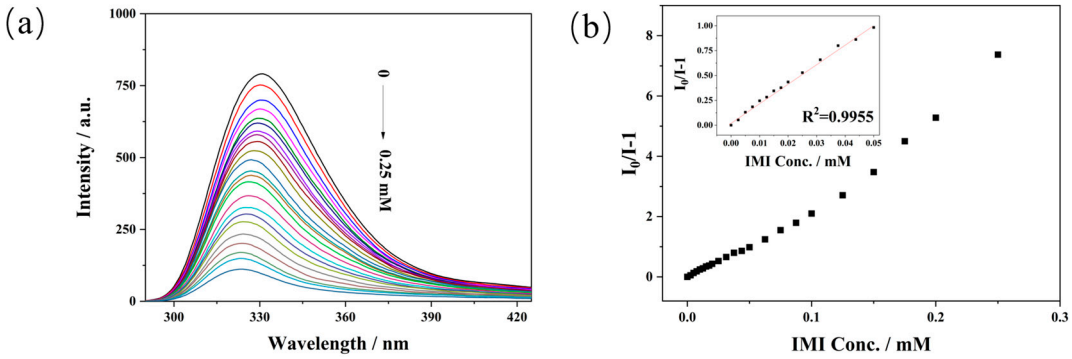

Figure S9. Fluorescence intensities of Complex Zn (a) dispersed in different concentrations of IMI; the plot of I_0/I - 1 of Complex Zn (b) *vs*. concentration of IMI in aqueous solution (Inset: The plot of I_0/I - 1 of the Complex Zn with the concentration over a IMI concentration range of 0 - 0.05 mM in aqueous solution).

Table S7. K_{sv} and LOD values for recently reported CP-based luminescence probes for IMI.

Sensor	Analyte	Concentration / mg·mL^{-1}	Linear range / μM	LOD / μM	$K_{sv} \times 10^4$ / M^{-1}	Ref.
Complex Zn	IMI	0.10	0-50	0.29	3.15	This work
$[Tb(PMBB)_{1.5}(H_2O)_2]$	IMI	1.00	0-100	0.26	3.01	[46]
$[Eu(PMBB)_{1.5}(H_2O)_2]$	IMI	1.00	0-100	0.29	2.63	[46]
$[Zn(BTC)(DTP)]\cdot(CH_3CN)_{1.5}\cdot(H_2O)_4$	IMI	0.10	0-50	2.51	3.05	[47]
$[Zn(DTP)SO_4(H_2O)_3]_n$	IMI	0.10	0-40	0.28	3.31	[48]

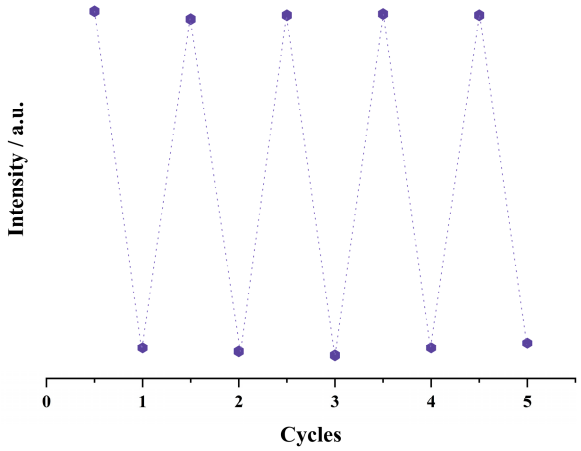

Figure S10. Recyclability of Complex Zn implemented with 1 mM MnO_4^- aqueous solution.

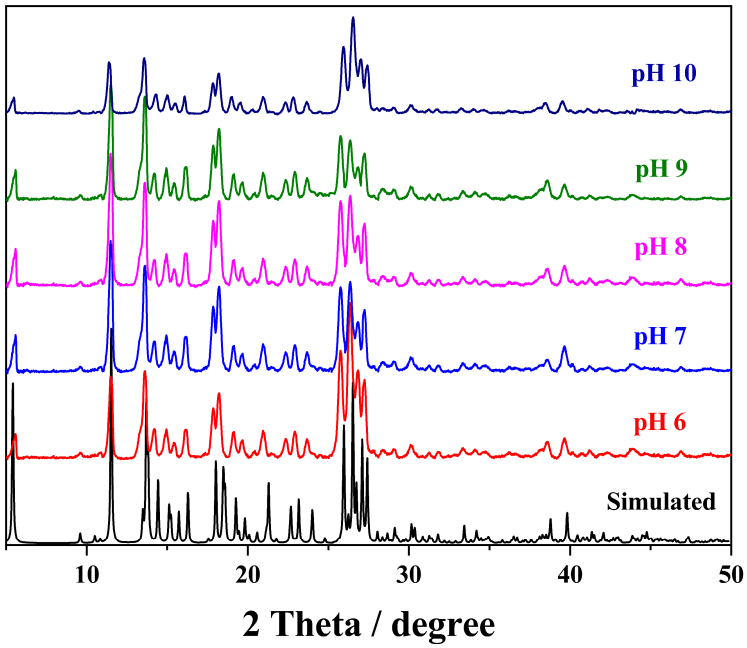

Figure S11. PXRD patterns of Complex Zn about pH resistance test: Complex Zn displayed strong stability in an aqueous solution with the pH values ranging from 6 to 10.

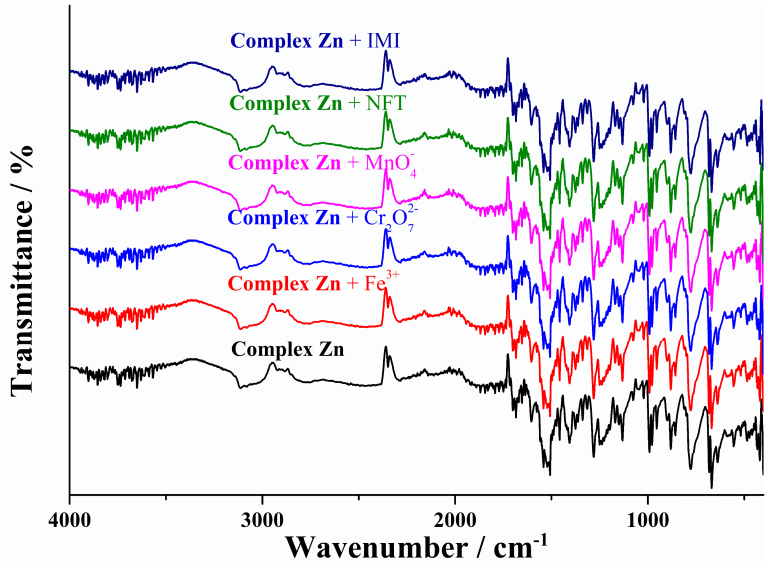

Figure S12. Comparison before and after adding test substance of FT-IR spectra of Complex Zn.

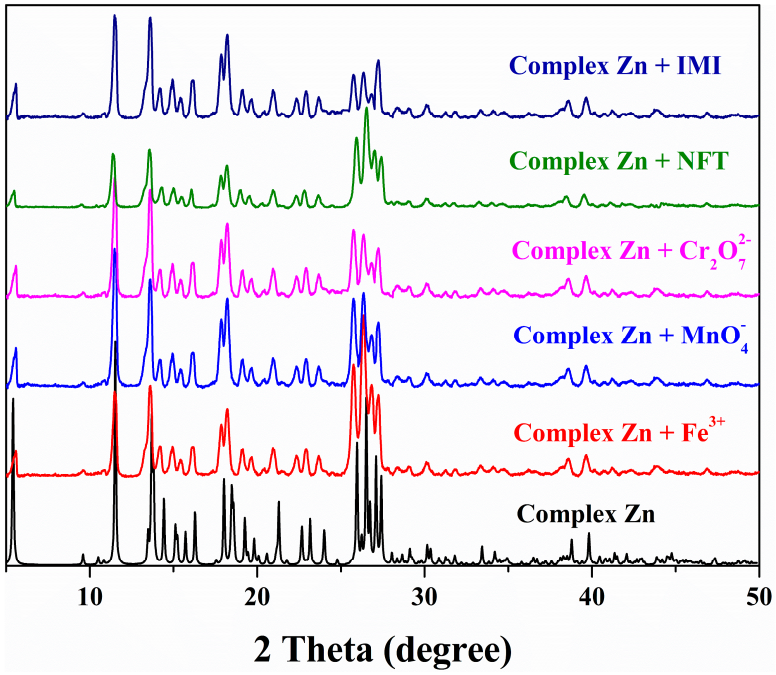

Figure S13. Comparison before and after adding test substance of PXRD patterns of Complex Zn.